Dependance of Linker Length and Composition on Ionic Conductivity and Lithium Deposition in Single-Ion Conducting Network Polymers

Michael L. Aubrey[a†], Jordan C. Axelson[a†], Kaitlyn E. Engler[b], Jeffrey R. Long[a–c]*

[a]Department of Chemistry, University of California, Berkeley, CA 94720, USA. Email: jrlong@berkeley.edu

[b]Department of Chemical and Biomolecular Engineering, University of California, Berkeley, CA 94720, USA.

[c]Materials Sciences Division, Lawrence Berkeley National Laboratory, Berkeley, CA 94720, USA.

† Authors contributed equally.

ABSTRACT: Single-ion conducting electrolytes stand as promising alternatives to state-of-the-art electrolytes in lithium batteries, although a single-ion conducting material with high Li^+ conductivity, stability in contact with lithium, and suitable mechanical properties has been slow to emerge. Here, we describe the synthesis of a series of single-ion conducting network polymers from the reaction of tetrakis(4-(chloromethyl)-2,3,5,6-tetrafluorophenyl)borate with oligoethylene glycoxide linkers $Li_2O[(CH_2CH_2)O]_n$ (n = 1, 2, 3, 9, and 22). Polymers with the longest linkers (n = 9 and 22; ANP-9 and ANP-10, respectively) form materials with conductivities of ~10^{-6} S cm^{-1} at 100 °C. With the addition of 65 wt % propylene carbonate (PC), all the network polymers in the series exhibit high conductivities at ambient temperatures, with the n = 1 material (ANP-6) achieving a bulk ionic conductivity of 2.5×10^{-4} S cm^{-1} at 25 °C. More conductive single-ion conducting gels could be prepared using the less coordinating pentanediol dilithium salt as a linker (ANP-11; $\sigma = 3.5 \times 10^{-4}$ S cm^{-1} at 25 °C), although this material exhibited a surprisingly high interfacial resistance in contact with a lithium electrode. In contrast, the gel formed with ANP-6 is notably stable in contact with metallic lithium electrodes, displays a lithium-ion transference number of unity, and boasts a wide electrochemical stability window of greater than 4.5 V. Temperature-dependent ac impedance analysis reveals that the ionic conductivity of this material—and likely the other gels in the series—matches closely to a Vogel-Tamman-Fulcher temperature model.

INTRODUCTION

State-of-the-art batteries rely on the reversible insertion of Li-ions into electrodes—typically carbon-based anodes and metal oxide cathodes—and feature liquid electrolytes consisting of lithium salts dissolved in organic solvents.[1,2] However, the consequent conduction of anions is not necessary for battery performance and can reduce cycling capacity, reduce cell lifetime (as the anions decompose at the electrodes), or worse, promote the dangerous growth of lithium dendrites.[3,4] Next generation lithium batteries will be expected to deliver greater energy densities, superior cycle efficiency, and improved safety.[5,6] However, achieving these goals requires the development of new electrolytes that exhibit enhanced stability and improved mechanical robustness while maintaining high ionic conductivities of at least 0.1 mS cm^{-1}. Additionally, novel electrolyte materials must be stable in contact with a lithium or lithium graphite anode and chemically inert toward strongly oxidizing cathodes (>4 V vs Li/Li^+).

While there are many opportunities for improving upon state-of-the-art lithium electrolytes,[7] one strategy for overcoming the challenges associated with mobile anions is to develop single-ion conducting electrolytes. In these systems, the anion is typically immobilized within an inorganic lattice, as in lithium ion conducting ceramics and glasses, or immobilized by chemically appending the anion to a polymer backbone, as in solid polymer and gel electrolytes.[8–11] Consequently, in such materials the conduction of Li^+ accounts for the whole of the ionic conductivity. Most organic-polymer single-ion conductors explored to date have incorporated weakly coordinating carboxylate, sulfonate, or bis((trifluoromethyl)sulfonyl)amide anions, while only a handful of studies have investigated the use of borate anions.[12–19] Tetraphenylborate is a particularly attractive anion, given that the low electronegativity of the tetrahedral boron allows for some polarization of the negative charge onto the adjacent phenyl rings. This attribute, in tandem with the large size difference between the tetraphenylborate anions and Li^+ ions, may facilitate conduction by discouraging ion pair formation and/or the assembly of ions into larger aggregates.[20]

Some of us recently reported the design of anionic network polymers (ANP) composed of anionic tetraphenylborate nodes and rigid aromatic linkers for use as single-ion conducting electrolytes.[15] These materials are derived from parent porous aromatic frameworks (PAFs) that predominantly featured neutral tetraphenylmethane nodes.[21–24] It was found that the incorporation of anionic borate nodes directly into the framework enabled inclusion of lithium cations, resulting in single-ion conductors with transference numbers, t_{Li+}, as high as 0.93.[15] Similar conductivities and high transference numbers have recently been reported in mesoporous covalent organic frameworks with pendant anions.[25] In comparison, lithium transference numbers for liquid electrolytes are, with rare exception,[26] less than 0.5.[27] Notably, use of a perfluorinated tetraphenylborate resulted in the material ANP-2 (Fig. 1) achieving a conductivity of 2.7×10^{-4} S cm^{-1} at 28 °C in the presence of only ~10 wt % plasticizer,

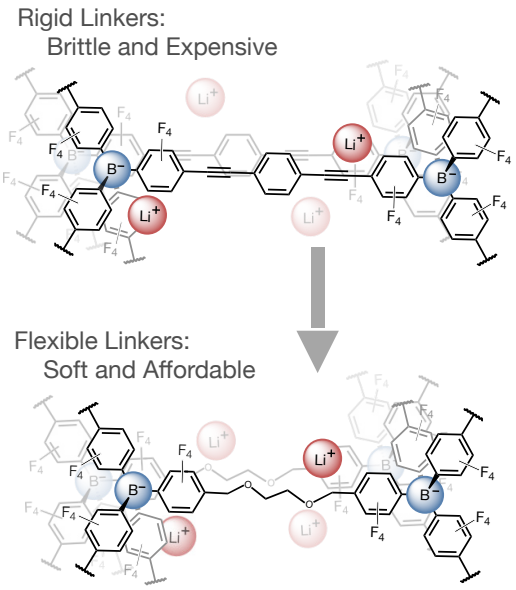

Figure 1. (Top) Structural model of our original PAF-based single-ion conducting anionic network polymers (ANP-2) featuring rigid linkers and synthesized using precious metal catalysts. (Bottom) Structural model of new ANPs developed in this work, featuring similar borate nodes connected by flexible linkers and prepared using a comparably inexpensive nucleophilic substitution route.

significantly less plasticizer than is required to achieve a comparable conductivity in typical gel and liquid electrolytes.

Despite the promising electrochemical properties of ANP-2, the material was mechanically brittle and difficult to shape into a format suitable for cell integration.[15] Moreover, the synthesis of ANP-2 utilized a palladium catalyst, rendering preparation of the material prohibitively expensive on an industrial scale. Here, we report a palladium-free synthesis of single-ion conducting polymer networks featuring fluorinated tetraphenylborate nodes and flexible oligo ethylene glycol linkers (Fig. 2).[28] Concomitant with this work, Shin *et. al.* have shown that this new synthetic route and class of polymers demonstrate great potential as solution castable materials, and they have employed the results of this study in the development of quasi-solid electrolyte film for lithium metal batteries.[29] Here, we illustrate how the length and composition of the flexible linkers affect the morphology, conductivity, and interfacial resistance of the electrolytes' contacts with a lithium electrode.

EXPERIMENTAL

The tetrafluoroborate monomer and ANP network polymers 6-11 were synthesized in the manner reported.[28,29] Methods and materials characterization can be found in the Supplementary Information.

Physical Measurements. Solution ^{1}H, ^{13}C, and ^{19}F NMR spectra were collected on a Bruker AV-300, AVQ-400, or AV-600 instrument and analyzed with MestReNova software (v.14.0.1-23559, Mestrelab Research S.L.). All resonances are referenced to the residual solvent signals of $CDCl_3$ (^{1}H, 7.26 ppm; ^{13}C, 77.2 ppm), MeCN-d_3 (^{1}H, 1.94 ppm; ^{13}C, 1.32 or 118 ppm), and $CFCl_3$ (^{19}F, 0 ppm). IR spectra were collected on a PerkinElmer Spectrum 400 FT-IR/FT-FIR Spectrometer. Mass spectrometry was performed at the QB3/Chemistry Mass Spectrometry Facility at the University of California, Berkeley using an orthogonal acceleration quadrupole time-of-flight (Q-tof) mass spectrometer with an electrospray ionization (ESI) source operated in negative ion mode (Q-tof Premier, Waters, Milford, MA). CHN elemental analyses were performed at the Microanalytical Laboratory of the University of California, Berkeley; lithium and chloride analysis was preformed at Galbraith Laboratories, Inc. Thermogravimetric analysis (TGA) was carried out at a ramp rate of 1 °C/m in a nitrogen flow using a TA Instruments Q5000 (Fig. S19–S24).

Electrochemical Sample Preparations. After drying the polymers at 120 °C on a Schlenk line, samples were transferred to an Ar glovebox. Pure polymers were analyzed as is. For conductivity measurements of materials containing plasticizer (anhydrous PC or triglyme), ~100 mg of polymer was weighed into a vial and a micropipette was used to add plasticizer in 10, 15, or 20 μL increments. After addition of plasticizer, the mixture was allowed to sit for 3 min and then agitated with a spatula in order to ensure equal distribution of plasticizer through the material prior to loading into a brass impedance cell. After each measurement, the pellet was returned to the sample vial and another aliquot of PC or triglyme was added and the process was repeated. Samples prepared for all other impedance and electrochemical measurements were loaded with PC and allowed to absorb the liquid over 15 h. Although the resulting materials could absorb at least 68 wt % PC, they remained free-flowing solids.

Ionic Conductivity Measurements. Electrochemical measurements were performed with a Bio-Logic VMP-3 multipotentiostat equipped with an impedance spectrometer. Impedance spectra were collected between 1 MHz and 1 Hz at 100 mV ac and temperature was recorded using a K-type thermocouple. Impedance measurements at and above ambient temperature were performed in a custom-built brass test cell (Fig. S25). Assembly of the cell was performed in the following manner. A Garolite spacer (thickness 0.25 mm) with a 3.88 mm diameter hole bored in the center was secured to a stainless-steel disk using Kapton tape. The disk was placed onto the base of the brass cell, and an insulating PEEK screw with a channel bored through its center was tightened onto the brass base, securing the plate and spacer. Subsequently, 4.0–5.5 mg of polymer material was loaded into the center of the spacer and a second stainless steel plate was pressed onto the top face of the sample. In this setup, stainless-steel plates function as blocking electrodes, and pellet contact is maintained between the two stainless steel electrodes with a 15-lb spring compressed between the brass cell caps.

Impedance spectra were fitted to the model circuit shown in Fig. S26 using the free software package EC-Lab by Bio-logic Inc. The ionic conductivity was then calculated from the refined cell resistance, R_{bulk}, using Equation 1 in which l is the pellet thickness, A is the electrode area, and σ_{bulk} is the bulk ionic conductivity of the sample in S cm^{-1}.

$$\sigma_{bulk} = \frac{A}{R_{bulk} l} \quad (1)$$

Molar conductivity was determined by measuring the sample volume using the same dimension measured to determine the ionic conductivity. After measuring the conductivity, the pellet mass was determined using a digital balance and the sample was dissolved in piranha solution. The quantity of lithium in the sample was then determined by ICP-OES. Finally, the lithium ion concentration was calculated using the mmol of Li^+ in the pellet and the geometric dimensions of the sample pellet.

Variable-Temperature Conductivity. Variable-temperature experiments were performed with a thermocouple inserted into the port at the base of the brass cell. Impedance measurements were taken every 5 °C from 30 to 100 °C. The resulting conductivity data were fit using the Stokes-Einstein relation[30] in order to determine an energy of activation. While the determination of these values is useful for comparison to other ion conductors at temperatures typically found during battery operation, measurements over a much larger temperature range were conducted also to determine the transport limiting mechanism of the materials as well. To this end, A two-electrode screw cell was packed with the sample in an Ar-filled glovebox and the sample was compressed until ionic conductivity measurements stabilized. The seams of the cell were sealed with Hysol 1C solventless epoxy that was allowed to set for 24 h. The cell was removed from the glovebox and the screws were attached to electrical leads at the end of a modified sample rod for a Quantum Design MPMS-XL. The assembly was then inserted into the sample chamber and the instrument cryostat was used to manually cool the cell in 10 K increments. The heating cycle was performed similarly with a 5 K offset from the cooling cycle. The Quantum Design MPMS-XL's built-in temperature controller was used to determine thermal equilibration.

Transference Number Determination. Lithium transference numbers were measured using the method of Evans, Bruce, and Vincent[30] with symmetric Li (s) | electrolyte | Li (s) cells formed by pressing polymer pellets between polished lithium metal on stainless steel current collectors. After equilibration of the cell at open circuit, a 100-mV dc bias was applied across the sample and the current response was recorded with time every 0.25 s. The steady state current (I_{ss}) was determined by fitting the resulting curve to an inverse square root time law Equation 2. An impedance spectrum was recorded immediately before the voltage step and at the end of the step. The transference number was then calculated using Equation 3 in which t_{Li+} is the transference number, I_0 is the initial current following the voltage step, ΔV is the dc voltage applied across the cell, R_0 is the charge transfer resistance for lithium reduction/oxidation measured by impedance spectroscopy before the voltage step, and R_{ss} is the resistance for lithium reduction/oxidation after reaching a steady state current.[31] Impedance spectra were fit to the model circuit in Fig. S27 using the software package EC-Lab, and the change in cell resistance was used to correct for changes in charge transfer resistance.

$$j(t) = \frac{c_1}{\sqrt{t+c_2}} + I_{ss} \quad (2)$$

$$t_{Li+} = \frac{I_{ss}(\Delta V - I_0 R_0)}{I_0(\Delta V - I_{ss} R_{ss})} \quad (3)$$

Cyclic Voltammetry. In a three-electrode cell constructed using a PFA union tee, lithium counter and reference electrodes were prepared atop stainless-steel current collectors. The cell body was filled with the electrolyte material and a stainless-steel working electrode was inserted to compress the electrolyte and complete the cell. The sweep rate was set to 0.1 mV/s to minimize cell polarization.

RESULTS AND DISCUSSION

To improve upon the structurally rigid ANP-2 (ANP = anionic network polymer) electrolyte, we sought to (i) avoid the use of a precious metal catalyst in synthesis, (ii) reduce material brittleness, and (iii) eliminate the need for organic solvents in

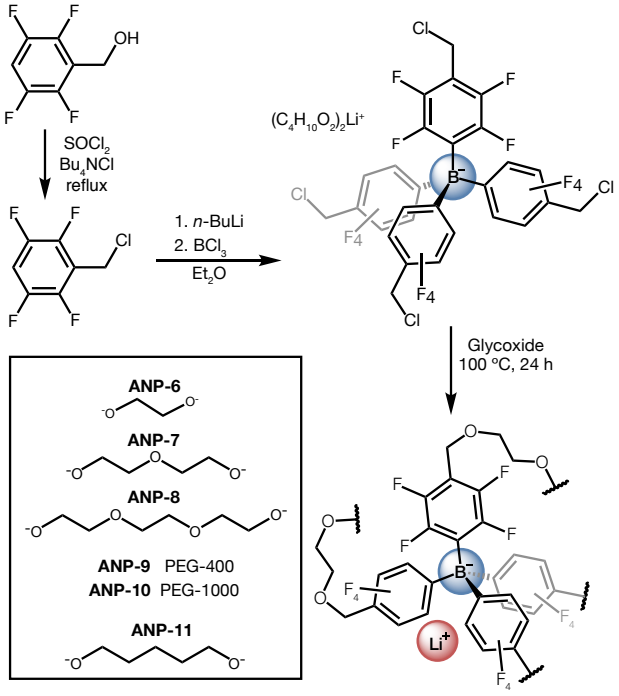

Figure 2. Synthesis of perfluorophenylborate network polymers. The inset shows each polymer name with the corresponding linker.

battery applications. Accordingly, we attempted to replace the rigid aromatic linker with flexible polyethylene glycol (PEG) linkers, which should ideally render the bulk material more amenable to film formation. Polyethylene glycols are commercially available and may be procured with a variety of electrophilic and nucleophilic end groups. Additionally, PEG is able to solvate lithium ions and is known to be stable in lithium polymer batteries.[2,7,32] Thus as a linker, PEG might facilitate Li^+ ion conduction in the absence of organic solvents. Furthermore, semicrystalline PEG-based polymer networks have shown some effectiveness in limiting the dendric growth of Li(*s*) in electrochemical cells.[33]

Nucleophilic substitution at the borate node was targeted as an alternative strategy to a palladium catalyzed cross-coupling for polymer synthesis. In considering a borate precursor suitable for this reaction, we sought to retain phenyl group fluorination while employing a reagent that would remain economically feasible for large-scale production. We ultimately chose 2,3,5,6-tetrafluorobenzyl alcohol for this purpose (Fig. 2), as it is already produced industrially as a precursor of the insecticide transfluthrin.[34,35]

A suitable route was initiated by converting the benzyl alcohol to the benzyl chloride, wherein the chloride would ultimately be used to attach a glycoxide linker through nucleophilic substitution. A solution of 2,3,5,6-tetrafluorobenzyl alcohol and tetrabutylammonium chloride in neat thionyl chloride was heated to reflux (Fig. 2), and total conversion to the benzyl chloride occurred in less than 1 h, as verified by ^{1}H NMR spectroscopy. The final product was isolated as a clear oil in excellent yield following purification by vacuum distillation. Selective deprotonation of 2,3,5,6-tetrafluorobenzyl chloride at the 4-position with *n*-butyllithium and subsequent reaction with boron trichloride resulted in formation of the corresponding tetraphenylborate. We note that this crude product must be thoroughly dried prior to centrifugation, as residual diethyl ether or

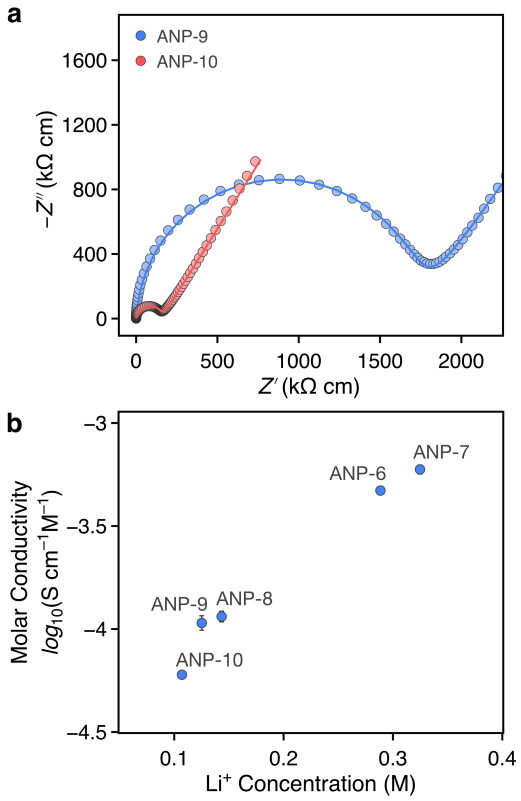

Figure 3. (a) Nyquist plots for the dry polymers ANP-9 and ANP-10 collected at 100 °C. Lines are fits to the data using the model circuit in Fig. S26. (b) Dependence of molar ionic conductivity in glycol-based ANP gels (65 wt% PC) on the concentration of lithium in the measured pellets.

dichloromethane increases its solubility in toluene and can dramatically reduce the isolated yield.

We screened a variety of reaction conditions for polymer formation with tri(ethylene glycol), including the reaction of our borate salt with the glycol in THF (ambient temperature and 65 °C), dimethoxyethane (85 °C), *N*,*N*-dimethyl formamide (100 °C), or dimethyl sulfoxide (100 °C). However, all these reaction conditions returned only starting materials. Alternatively, deprotonation of the glycol with *n*-butyllithium in 1,4-dioxane followed by addition of the borate and heating at 100 °C for 24 h yielded an insoluble, gelatinous material. No starting materials were identified in the ^{1}H NMR spectrum of the reaction supernatant, and near complete disappearance of strong bands in the C–Cl frequency range (800–600 cm^{-1}) of the IR spectrum of the dried product indicated loss of benzyl chloride (Fig. S18). Elemental analysis is also consistent with ~90% substitution of the benzylic chlorides (see experimental). Optimization of the reaction conditions enabled the isolation of five polymers with varying PEG chain lengths as yellow or tan solids: ANP-6 (ethylene glycol, 61% yield), ANP-7 (di(ethylene glycol), 87%), ANP-8 (tri(ethylene glycol), 90%), ANP-9 (poly(ethylene glycol)-400, 72%), and ANP-10 (poly(ethylene glycol)-1000, 36%). The lower yield for ANP-10 is likely because this material forms small particles that are decanted during purification in addition to the bulk film.

The polymers are insoluble in common organic solvents such as dichloromethane, ethers, acetonitrile, acetone, methanol, and dimethyl sulfoxide, and are accordingly readily isolated and purified by decanting and solvent washing (see Experimental Section). Polymer synthesis in the absence of stirring results in the formation of a homogenous gelatinous film in all cases. However, drying the washed polymers at 120 °C for 12 h leads to powder formation in the case of ANP-6, ANP-7, and ANP-8, while polymers ANP-9 and ANP-10 remain intact as rubbery flakes. Over the course of the study, it became apparent that these materials were not appropriate for film preparation. As shown by Shin *et al.*,[29] additional tailoring of the linker would be needed for interparticle cross-linking in order to form robust films. TGA analyses show ANP-6, ANP-7, and ANP-8 are stable up to about 300°C. ANP-9, and ANP-10 are stable up to about 250°C. However, the decomposition onset for ANP-11 is significantly lower at about 180°C (Fig. S19–S24).

The subsequent conductivity studies utilized polymer as pressed pellets of powder (ANP-6, ANP-7, and ANP-8) or flaky solid (ANP-9, ANP-10) formed from quiescent solutions. Interestingly, we find that ANP-6, ANP-7 and ANP-8 are not conductive as pure solids, while ANP-9 and ANP-10 only display low conductivities at 100 °C (5.5×10^{-7} S cm^{-1} and 6.3×10^{-6} S cm^{-1}, respectively, Fig. 3a), although the conductivity of ANP-10 is measurable at 30 °C (7.2×10^{-8} S cm^{-1}, Fig. S28). The higher conductivity of ANP-10 may be a result of the longer, more flexible linkers, which can promote segmental motion of the solvating ethylene glycol chains and in turn facilitate Li^+ ion mobility through the bulk material.[16] Variable-temperature conductivity data for ANP-9 and ANP-10 between 30 °C and 100 °C was modelled using the Stokes- Einstein relation, yielding activation energies for Li^+ hopping of 1.30 and 0.66 eV, respectively. These values are high relative to the previously reported value of 0.25 eV for ANP-2,[15] although comparable to values typically observed for other solid polymer electrolytes.[36]

We sought to further improve ionic conductivity in the materials through the addition of propylene carbonate (PC) or triglyme as plasticizers.[37,38] For the neat polymers, the ethylene glycol linkers serve to solvate Li^+, but their motion can be inhibited by ionic cross-linking within the material. The addition of plasticizer can provide better solvation of Li^+, disrupt ionic cross linking, and reduce ion pairing by dissociation of Li^+ from the ANP backbone.[16,39] With the addition of either PC or triglyme, the polymers' particles swell noticeably, an effect that may improve interparticle contacts and corresponding conductivity of the materials in pellet form. For ANP-6 and ANP-7, we found that that the polymer loaded with PC was slightly more conductive than the material loaded with triglyme (Fig. 4a and Fig. S31), and a maximum conductivity was achieved at 65–69 wt% PC (Fig. 4b). Thus, these materials are best described as single-ion conducting polymer gels rather than solid polymer electrolytes. The plateau in conductivity above ~60 wt % plasticizer in Fig. 4a is consistent with the formation of a highly interconnected network polymer, which should limit further volumetric expansion of the material.

While only the polymers featuring longer linkers were conductive as neat solids, all the polymers loaded with 65 wt % PC displayed significant conductivity at room temperature. Molar conductivities were estimated by measuring the volume of the conductivity samples then digesting them for elemental analysis. These measurements revealed a monotonic increase in molar conductivity with increasing ion concentration (Fig. 3b) and supports a scenario where bulk conductivity is limited by ion mobility rather than by lithium-ion concentration. This trend is also consistent with the fact that shortening the linker

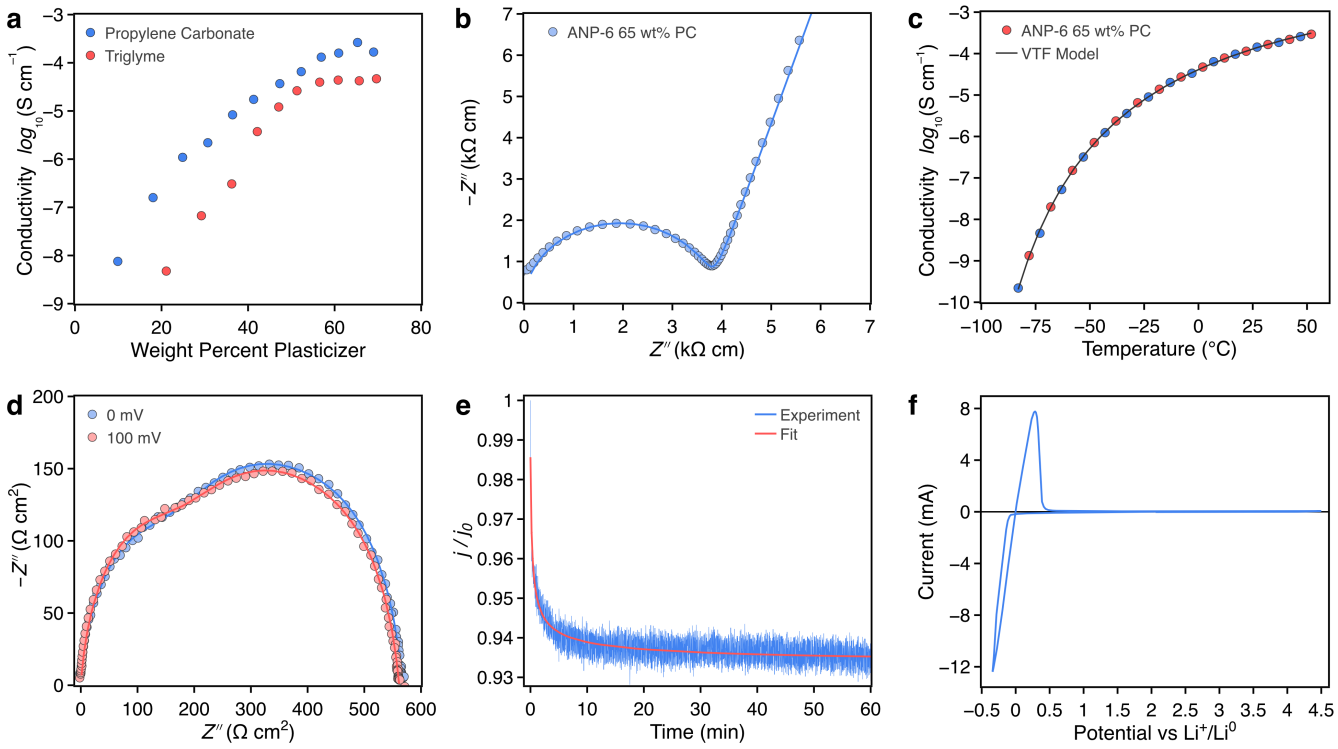

Figure 4. Electrochemical characterization of ANP-6 and 65 wt % PC. (a) The dependence of ionic conductivity on the inclusion of plasticizers PC and triglyme at room temperature. (b) Nyquist plot for the material at room temperature fit to the model circuit in Figure S26. (c) Variable temperature conductivity collected between 190 and 325 K, fit to the Vogel-Tamman-Fulcher model. Blue points were collected while cooling and red points were collected while heating the sample back to room temperature. (d) Nyquist plots for a Li| ANP-6 at 65 wt % PC|Li cell at open circuit voltage before polarization and at 100 mV dc after obtaining a steady state current. Data are fit to the model circuit in Figure S27. (e) Potentiostatic polarization curve complementing the Nyquist plots in (e) fit to a Fickian diffusion model. (f) Cyclic voltammogram of the material collected using a stainless-steel working electrode, lithium counter and reference electrodes and a scan rate of 0.1 mV.

effectively increases the relative concentration of Li^+ and shortens the effective hopping distance. Attempts to further increase the concentration of Li^+ by adding 1 M TFSI in PC to ANP-6 and ANP-7 afforded only relatively small increases in ionic conductivity (Fig. S32).

With the addition of PC, we hypothesized the coordinating properties of PEG are no longer necessary to solvate the polymer. In fact, interactions between Li^+ and the ether groups could potentially hinder ion transport by localizing Li^+ on the ANP backbone. To test if conductivity could be improved by reducing the number of coordinating moieties in the linker, we prepared another polymer, ANP-11, with 1,5-pentanediol as the linker. The 1,5-pentanediol is analogous to the linker in ANP-7 but features a non-coordinating methylene group in place of an ether. Notably at 65 wt % PC, the ANP-11 gel exhibited a conductivity of 3.5×10^{-4} S cm^{-1}—a more than two-fold enhancement in conductivity compared to ANP-7 with the same amount of plasticizer.

Variable-temperature conductivity data were collected for ANP-6, ANP-7, and ANP-11 in the presence of 65 wt % PC to determine the Arrhenius energy for Li^+ ion conduction (Table 1, and Fig. S30). Fits to the data employing the Stokes-Einstein relation yielded activation energies of 0.22 and 0.24 eV for ANP-6 and ANP-7, respectively. Though slight, this difference is consistent with ANP-6 possessing a higher concentration of Li^+. Interestingly, the activation energy for ANP-11 is also 0.22 eV, slightly lower than that of ANP-7, even though the constituent two linkers have similar length.

While a comparison of activation energies is useful to evaluate electrolyte performance near ambient operating conditions, conductivity measurements over such a small temperature range (30–100 °C) are insufficient for distinguishing an ion hopping mechanism from other transport models. To this end, variable-temperature conductivity data were collected for ANP-6 with a 65 wt % PC loading for temperatures as low as –83 °C (Fig. 4c). The data was best fit using a Vogel-Tamman-Fulcher model for ionic conductivity and are consistent with bulk transport limited by the effective viscosity of the electrolyte.[40–42] This transport limiting phenomenon is typical for liquids,

Table 1. Polymers and corresponding ionic conductivities with inclusion of 65 wt % PC.

Name	Linker	Length (*n*)	wt % Li^+ [a]	Log(σ) (S cm^{-1})	EA (eV)
ANP-6	Ethylene glycol	2	0.23	−3.60	0.22
ANP-7	Diethylene glycol	5	0.24	−3.80	0.24
ANP-8	Triethylene glycol	8	0.23	−4.51	-
ANP-9	PEG-400	26	0.16	−4.78	-
ANP-10	PEG-1000	65	0.14	−4.58	-
ANP-11	Pentanediol	5	0.23	−3.46	0.22

[a]Based on the mass of the dry polymer

gels, and polymer electrolytes above their glass transition temperatures.

The two materials with the highest ambient temperature conductivities, ANP-6 and ANP-11, were sufficiently conductive for the determination of their stabilities in contact with lithium electrodes, transference numbers, and electrochemical stability windows. We accordingly constructed symmetric Li(s) | electrolyte | Li(s) cells in which the electrolyte consisted of an ANP and 65 wt % PC. Although ANP-11 is more conductive than ANP-6, it formed a surprisingly resistive interface with the lithium electrodes (~10,000 Ω cm^{-2}), precluding further analysis. Cells constructed with the ANP-6 electrolyte demonstrated more reasonable, area specific, charge transfer resistances. As a result of the non-blocking Li-metal electrodes, two relaxation processes are observed for the cell (Fig. 4d) and these could be modelled using the circuit in Fig S27 as a high-frequency feature assigned to the bulk ionic conductivity of the electrolyte and a low-frequency feature assigned to charge transfer resistance for Li^+ plating at the electrodes. Time-dependent impedance analysis in the 16 hours following cell assembly (Fig. S33) revealed a settling of the bulk electrolyte ionic conductivity and some evolution of the charge transfer resistance at the lithium-electrolyte interfaces. Both processes eventually stabilize after ~6 h. Importantly, the charge transfer resistance does not increase over time, indicating that ANP-6 mixed with 65 wt % PC is stable in contact with lithium. Given the structural similarity between ANP-6 and ANP-11, we hypothesize that poor wettability of the nonpolar hydrocarbon linkers in ANP-11 with the solid-electrolyte interphase is the primary factor inhibiting conductivity in the battery prototype for this material.

To determine the lithium-ion transference number for the ANP-6 electrolyte, we used the potentiostatic polarization method proposed by Bruce, Evans, and Vincent.[31] First, a small potential was applied across the symmetric cell and the dc current response was recorded (Fig. 4e). For common liquid electrolytes, the current decays by 60–70% due to the ancillary conduction of anions forming a concentration gradient in the cell. In contrast, for a single-ion conductor the change between the initial (I_0) and steady state current (I_{ss}) values should be negligible. For ANP-6 with 65 wt % PC, the current decays by only ~6% following a Fickian time dependence. Fig. 4d shows the impedance spectra before the potential step was applied and after a steady-state current was reached. From the impedance spectra, non-ohmic changes in the charge transfer rates at the lithium electrodes are corrected for by comparison of the impedance spectra at zero field (R_0) and non-zero field (R_{ss}). Ultimately, using Equation 3, we determined t_{Li+} to be 1.01(1) for ANP-6.

The electrochemical stability window of ANP-6 with 65 wt % PC was determined using a three-electrode cell with lithium reference and counter electrodes and a stainless-steel working electrode (Fig. 4f). Reversible deposition and dissolution of lithium on the working electrode was observed as expected at ~0 V versus Li/Li^+, and the electrolyte displays good oxidative stability up to 4.5 V, consistent with the immobilization of anions in the polymer network. A very small increase in oxidative current is observed above 3.0 V and may stem from the redox activity of transition metal cations on the stainless-steel surface. This large electrochemical stability potentially qualifies ANP-6 as a candidate electrolyte for use with high voltage metal–oxide cathodes.

CONCLUSIONS

Five new perfluorotetraphenyl borate-based single-ion conducting polymer electrolytes with flexible linkers were synthesized via a scalable and inexpensive route. Two of these materials, ANP-9 and ANP-10 (featuring PEG-400 and PEG-1000 linkers, respectively) form as pliable flakes and are conductive in the absence of plasticizer, although their conductivities (~10^{-6} S cm^{-1} at 100 °C) are too low for practical battery applications. With the addition of 65 wt % PC plasticizer, the conductivity of ANP-9 and ANP-10 increases by an order of magnitude, while shorter chain polymers ANP-6, ANP-7, ANP-8 and ANP-11 also form gel polymer electrolytes with significantly higher conductivities (~10^{-4} S cm^{-1}) at room temperature. Importantly, ANP-6 shows good stability toward Li-metal electrodes, a lithium transference number of unity, and a large electrochemical stability window.

Conflicts of interest

The materials describe here are also the subject of US Patent Application #16049911.

Acknowledgements

Quantification of the lithium content of the materials was supported as part of the Joint Center for Energy Storage Research, an Energy Innovation Hub funded by the U.S. Department of Energy, Office of Science, Basic Energy Sciences. All other aspects of this research were supported by Robert Bosch, LLC through a Bosch Energy Research Network (BERN) grant. We thank the National Science Foundation for support of J.C.A. through Graduate Research Fellowship Grant No. DGE-1106400, Prof. Jeffrey F. Van Humbeck for synthetic direction, and Prof. Zachary Smith for characterization advice. Support in screening reaction conditions for 2,3,5,6-tetrafluorobenzyl chloride was provided by Prof. Robert G. Bergman's Spring 2015 CHEM 115 class (Kersti Caddell Haatveit, Tiffany Chen, Khaled Jami, and Zhenfeng Yu) and experimental assistance was provided by Brittany Gomez. We thank Dr. Katie Meihaus for editorial assistance.

ASSOCIATED CONTENT

Supporting Information

The Supporting Information is available free of charge on the ACS Publications website.

Synthetic procedures, NMR, FT-IR, ESI mass spectrometry, thermogravimetric analysis, and impedance spectra. (PDF)

AUTHOR INFORMATION

Corresponding Author

* Correspondence should be addressed to Jeffrey R. Long; email: jrlong@berkeley.edu

Author Contributions

The manuscript was written through contributions of all authors. All authors have given approval to the final version of the manuscript. †These authors contributed equally.

REFERENCES

(1) Jow, T. R.; Xu, K.; Borodin, O.; Ue, M. *Electrolytes for Lithium and Lithium-Ion Batteries*; Modern Aspects of Electrochemistry; 2014; Vol. 58.

(2) Xu, K. Nonaqueous Liquid Electrolytes for Lithium-Based Rechargeable Batteries. *Chem. Rev.* **2004**, *104* (10), 4303–4418.

(3) Chazalviel, J. N. Electrochemical Aspects of the Generation of Ramified Metallic Electrodeposits. *Phys. Rev. A* **1990**, *42* (12), 7355–7367.

(4) Rosso, M.; Gobron, T.; Brissot, C.; Chazalviel, J. N.; Lascaud, S. Onset of Dendritic Growth in Lithium/Polymer Cells. *J. Power Sources* **2001**, *97–98*, 804–806.

(5) Armand, M.; Tarascon, J.-M. Building Better Batteries. *Nature* **2008**, *451*, 652–657.

(6) Blomgren, G. E. The Development and Future of Lithium Ion Batteries. *J. Electrochem. Soc.* **2017**, *164* (1), A5019–A5025.

(7) Quartarone, E.; Mustarelli, P. Electrolytes for Solid-State Lithium Rechargeable Batteries: Recent Advances and Perspectives. *Chem. Soc. Rev.* **2011**, *40* (5), 2525–2540.

(8) Bouchet, R.; Maria, S.; Meziane, R.; Aboulaich, A.; Lienafa, L.; Bonnet, J.-P.; Phan, T. N. T.; Bertin, D.; Gigmes, D.; Devaux, D.; Denoyel, R.; Armand, M. Single-Ion BAB Triblock Copolymers as Highly Efficient Electrolytes for Lithium-Metal Batteries. *Nat. Mater.* **2013**, *12* (5), 452–457.

(9) Lian, F.; Guan, H.; Wen, Y.; Pan, X. Polyvinyl Formal Based Single-Ion Conductor Membranes as Polymer Electrolytes for Lithium Ion Batteries. *J. Membr. Sci.* **2014**, *469*, 67–72.

(10) Sumathipala, H. H.; Hassoun, J.; Panero, S.; Scrosati, B. High Performance PEO-Based Polymer Electrolytes and Their Application in Rechargeable Lithium Polymer Batteries. *Ionics* **2007**, *13* (5), 281–286.

(11) Sun, X. New Gel Polyelectrolytes for Rechargeable Lithium Batteries. *Solid State Ion.* **2004**, *175* (1–4), 713–716.

(12) and, X.-G. S.; Kerr, J. B. Synthesis and Characterization of Network Single Ion Conductors Based on Comb-Branched Polyepoxide Ethers and Lithium Bis(Allylmalonato)Borate. *Macromolecules* **2005**, *39* (1), 362–372.

(13) Cakmak, G.; Verhoeven, A.; Jansen, M. Synthesis and Characterization of Solid Single Ion Conductors Based on Poly[Lithium Tetrakis(Ethyleneboryl)Borate]. *J. Mater. Chem.* **2009**, *19* (25), 4310–4318.

(14) Driscoll, P. F.; Yang, L.; Gervais, M.; Kerr, J. B. Polyelectrolyte Membranes Containing Lithium Malonato(Difluoro)Borate for Lithium-Ion Systems. *ECS Trans.* **2011**, *33* (23), 33–53.

(15) Humbeck, J. F. V.; Aubrey, M. L.; Alsbaiee, A.; Ameloot, R.; Coates, G. W.; Dichtel, W. R.; Long, J. R. Tetraarylborate Polymer Networks as Single-Ion Conducting Solid Electrolytes. *Chem Sci* **2015**, *6* (10), 5499–5505.

(16) Sun, X.-G.; Reeder, and C. L.; Kerr, J. B. Synthesis and Characterization of Network Type Single Ion Conductors. *Macromolecules* **2004**, *37* (6), 2219–2227.

(17) Wang, X.; Liu, Z.; Kong, Q.; Jiang, W.; Yao, J.; Zhang, C.; Cui, G. A Single-Ion Gel Polymer Electrolyte Based on Polymeric Lithium Tartaric Acid Borate and Its Superior Battery Performance. *19th Int. Conf. Solid State Ion.* **2014**, *262*, 747–753.

(18) Xu, G.; Zhang, Y.; Rohan, R.; Cai, W.; Cheng, H. Synthesis, Characterization and Battery Performance of A Lithium Poly (4-Vinylphenol) Phenolate Borate Composite Membrane. *Electrochimica Acta* **2014**, *139*, 264–269.

(19) Zhu, Y. S.; Gao, X. W.; Wang, X. J.; Hou, Y. Y.; Liu, L. L.; Wu, Y. P. A Single-Ion Polymer Electrolyte Based on Boronate for Lithium Ion Batteries. *Electrochem. Commun.* **2012**, *22*, 29–32.

(20) Liang, S.; Choi, U. H.; Liu, W.; Runt, J.; Colby, R. H. Synthesis and Lithium Ion Conduction of Polysiloxane Single-Ion Conductors Containing Novel Weak-Binding Borates. *ACS Publ.* **2012**, *24* (12), 2316–2323.

(21) Ben, T.; Qiu, S. Porous Aromatic Frameworks: Synthesis, Structure and Functions. *CrystEngComm* **2013**, *15* (1), 17–26.

(22) Ding, S.-Y.; Wang, W. Covalent Organic Frameworks (COFs): From Design to Applications. *Chem. Soc. Rev.* **2013**, *42* (2), 548–568.

(23) Fischer, S.; Schmidt, J.; Strauch, P.; Thomas, A. An Anionic Microporous Polymer Network Prepared by the Polymerization of Weakly Coordinating Anions. *Angew. Chem. Int. Ed.* **2013**, *52* (46), 12174–12178.

(24) Zhu, G.; Ren, H. *Porous Organic Frameworks*; Springer Berlin Heidelberg; Springer Berlin Heidelberg, 2015.

(25) Hu, Y.; Dunlap, N.; Wan, S.; Lu, S.; Huang, S.; Sellinger, I.; Ortiz, M.; Jin, Y.; Lee, S.; Zhang, W. Crystalline Lithium Imidazolate Covalent Organic Frameworks with High Li-Ion Conductivity. *J. Am. Chem. Soc.* **2019**,

(26) Wong, D. H. C.; Thelen, J. L.; Fu, Y.; Devaux, D.; Pandya, A. A.; Battaglia, V. S.; Balsara, N. P.; DeSimone, J. M. Nonflammable Perfluoropolyether-Based Electrolytes for Lithium Batteries. *Proc. Natl. Acadamy Sci. USA* **2014**, *111* (9), 3327.

(27) *Encyclopedia of Applied Electrochemistry*; Springer New York; Springer New York, 2014.

(28) Axelson, J. C. From Coordination Complexes to Conductive Polymers: The Synthesis and Characterization of Anionic Molecules and Materials. Ph.D. Dissertation, University of California Berkeley, Berkeley, CA, 2016.

(29) Shin, D.; Bachman, J. E.; Taylor, M. K.; Kamcev, J.; Park, J. G.; Ziebel, M. E.; Velasquez, E.; Jarenwattananon, N. N.; Sethi, G. K.; Cui, Y.; Long, J. R. A Single-Ion Conducting Borate Network Polymer as a Viable Quasi-Solid Electrolyte for Lithium Metal Batteries. *Adv. Mater.* **2020**, *32* (10), 1905771.

(30) Linford, R. G.; Hackwood, S. Physical Techniques for the Study of Solid Electrolytes. *Chem. Rev.* **1981**, *81* (4), 327–364.

(31) Bruce, P. G.; Evans, J.; Vincent, C. A. Conductivity and Transference Number Measurements on Polymer Electrolytes. *Solid State Ion. 19 Proc. 19th Int. Conf. Solid State Ion.* **1988**, *28–30*, 918–922.

(32) Agrawal, R. C.; Pandey, G. P. Solid Polymer Electrolytes: Materials Designing and All-Solid-State Battery Applications: An Overview. *J. Phys. Appl. Phys.* **2008**, *41* (22), 223001.

(33) Zheng, Q.; Ma, L.; Khurana, R.; Archer, L. A.; Coates, G. W. Structure–Property Study of Cross-Linked Hydrocarbon/Poly (Ethylene Oxide) Electrolytes with Superior Conductivity and Dendrite Resistance. *Chem. Sci.* **2016**, *7* (11), 6832–6838.

(34) Paranjape, K.; Gowariker, V.; Krishnamurthy, V. N.; Gowariker, S. *The Pesticide Encyclopedia.*; CABI; CABI, 2015.

(35) WHO Specifications and Evaluations for Public Health Pesticides: Transfluthrin. *World Health Organ.* **2006**, 20.

(36) Fergus, J. W. Ceramic and Polymeric Solid Electrolytes for Lithium-Ion Batteries. *J. Power Sources* **2010**, *195* (15), 4554–4569.
(37) Meyer, W. H. Polymer Electrolytes for Lithium-Ion Batteries. *Adv. Mater.* **1999**, *10* (6), 439–448.
(38) Xu, W.; Angell, C. A. Polymer Electrolytes from Plasticized PolyMOBs and Their Gel Forms. *Electrochimica Acta* **2003**, *48* (14), 2029–2035.
(39) Choi, U. H.; Liang, S.; O'Reilly, M. V.; Winey, K. I.; Runt, J.; Colby, R. H. Influence of Solvating Plasticizer on Ion Conduction of Polysiloxane Single-Ion Conductors. *Macromolecules* **2014**, *47* (9), 3145–3153.
(40) Fulcher, G. S. Analysis of Recent Measurements of the Viscosity of Glasses. *J. Am. Ceram. Soc.* **1925**, *8* (6), 339–355.
(41) Tammann, G.; Hesse, W. Die Abhängigkeit Der Viscosität von Der Temperatur Bie Unterkühlten Flüssigkeiten. *Z Anorg Allg Chem* **1926**, *156* (1), 245–257.
(42) Vogel, H. The Law of the Relation between the Viscosity of Liquids and the Temperature. *Phys Z* **1921**, *22*, 645–646.

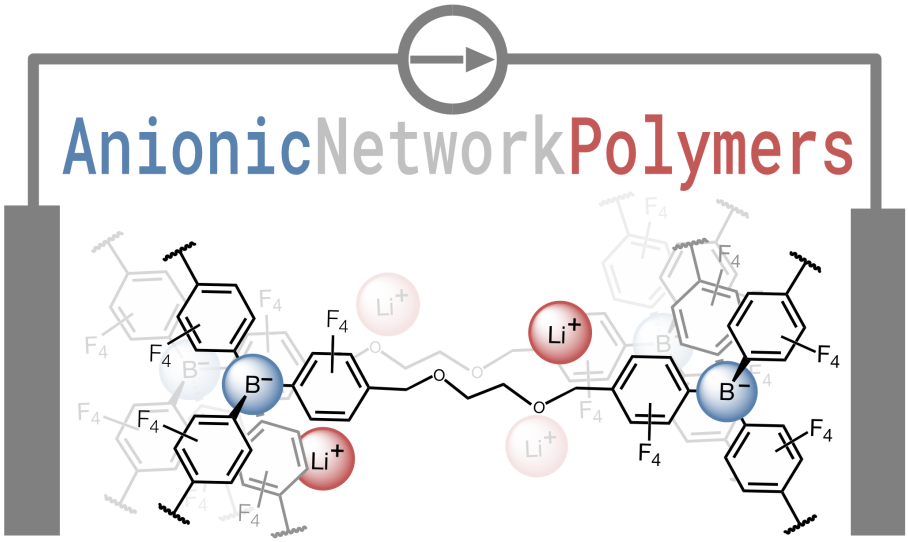
AnionicNetworkPolymers
Li+
Li+
Li+
B−
B−
F4